Wetting of a glass substrate by a binary liquid mixture

Xiao-lun Wu, Mark Schlossman, and Carl Franck
Laboratory of Atomic and Solid State Physics and Materials Science Center, Cornell University, Ithaca, New York 14853
(Received 13 June 1985)

By reflecting light from a horizontal solid-liquid interface, we have measured the thickness of a gravity-thinned wetting layer in a stirred binary liquid as a function of temperature. The binary liquid studied is a mixture of polar and nondipolar liquids, nitromethane and carbon disulfide, respectively. At coexistence the lighter bulk nitromethane-rich (N^*) phase floats above the heavier carbon-disulfide–rich (C^*) phase. It is observed along the coexistence curve, while the liquid is stirred by a floating glass magnetic mixer, that a thick wetting layer of the N^* phase starts to develop on the borosilicate glass substrate at the bottom of the sample cell about 150 mK below the bulk critical temperature T_c. The wetting layer thickness, which is about 400 nm (the height spanned by the C^* phase is 0.82 cm), becomes constant through 7 K below T_c, while in the temperature range $T_c - T < 150$ mK, the layer thickness is greatly reduced. Upon approaching bulk coexistence (off the critical composition) in the C^* region, the N^* wetting layer increases in thickness as is expected for a retarded van der Waals interaction.

I. INTRODUCTION

These wetting experiments grew out of the observation that a binary liquid mixture of nitromethane and carbon disulfide develops a thick wetting layer of the gravitationally unfavored phase, i.e., a nitromethane-rich (N^*) phase, on a horizontal borosilicate glass substrate when the system is cooled from the one-phase region onto bulk coexistence. Recently we discovered that such a quenched wetting layer in a system at coexistence thins to a steady-state thickness when the sample is stirred at a fixed temperature. The thickness of such a layer was found to remain constant over a period of 36 h ($T_c - T = 7$ K). Kayser, Moldover, and Schmidt[1] suggest for the first time the role of stirring in determining the steady-state thickness of the wetting layer in these phase-separated samples. At bulk coexistence we found that a steady-state wetting layer can be easily burnt away by slightly raising the temperature of the water bath surrounding the sample cell. Subsequently, if the sample is stirred and the temperature fixed, the system recovers to its original steady-state thickness. Similarly, if a sample at bulk coexistence is quenched, i.e., lowered in temperature, the wetting-layer thickness is increased beyond the steady-state value. If the sample is not stirred, the enhanced wetting-layer thickness was observed to persist for more than 12 h ($T_c - T = 2$ K). Continuous stirring returned the layer to its original thickness. The wetting-layer recovery times for quenched or burned systems at coexistence that are continuously stirred varied from a few hours near the critical point to on the order of days far from T_c. Typical recovery measurements are shown in Fig. 1. The wetting layers were smooth and stable while the sample cell was inside the thermostat (temperature drift of 0.2 mK/week). Measurements were also performed while the system was in the bulk single-phase region and off the critical concentration. Here the recovery behavior of the reflectivity was like that observed in our critical adsorption experiments,[2] i.e., long recovery times were not noticed. The purpose of this report is to present these new observations of wetting at fixed temperatures.

Wetting phenomena have been studied theoretically by many workers, including Cahn[3(a)] and Nakanishi and Fisher.[3(b)] Using a Landau-Ginzburg expansion for the free energy with a short-range contact interaction, Nakanishi and Fisher mapped out the phase diagrams for a semi-infinite system. According to their theory, complete wetting (characterized by an infinitely thick film) occurs only when H_1 (the surface field) and H (the bulk field) have different signs while H approaches zero. A prewetting (PW) line was predicted, which takes off tangentially from the bulk coexistence curve at the wetting transition

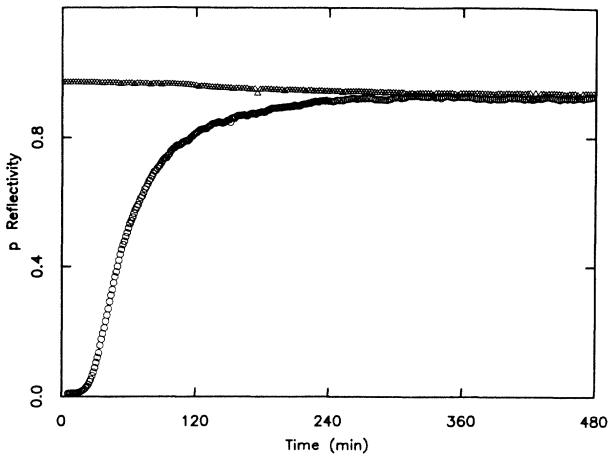

FIG. 1. Reflectivity recovery curves at coexistence. Triangles are reflectivity measurements after cooling (at a rate of 100 mK/min) and circles are reflectivity measurements after heating (at a rate of 50 mK/min). The light is p polarized. Measurements are at $T - T_c \approx -3$ K, with the final temperatures for the two experiments differing by T(heating, final) $-$ T(cooling, final) $= 0.1$ K. The final temperature was attained in approximately 5 min from time zero.

point (WP, temperature T_w) and terminates at a prewetting critical point (PWC) in the bulk one-phase region. A hypothetical phase diagram for our system is shown in Fig. 2(a). Along the prewetting line a first-order low-adsorption—high-adsorption transition is expected, except at PWC, where the transition becomes continuous. Using a perturbative approach, Privman[3(c)] has taken long-range van der Waals forces into consideration. One of his interesting findings is that when the long-range liquid substrate interaction favors a change in the order parameter (chemical concentration) in the same direction as H_1 and for $T > T_w$, complete wetting may still result. In this case, as the system approaches the bulk coexistence curve, the wetting-layer thickness h grows as $h \propto H^{-q}$, where nonretarded and retarded van der Waals forces give $q = \frac{1}{3}$ and $\frac{1}{4}$, respectively, in analogy to gas adsorption on a solid.[3(c),3(d)] On the other hand, if the long-range liquid-substrate interaction is opposed to the surface field H_1, complete wetting is suppressed, resulting in a finite wetting-layer thickness; see also Ref. 3(e). In reality, even when the system is completely wet the layer thickness may not be on the order of the sample-cell size. As pointed out by de Gennes[3(f)] and Lipowsky,[3(g)] an infinite wetting-layer thickness can be destabilized by gravity. In the gravity-thinned wetting system, assuming that there is no stirring as shown in Fig. 2(b), the wetting-layer thickness h at bulk coexistence is given by[3(f),3(g)]

$$h = (2W/\Delta\rho g L)^q , \tag{1}$$

where W is the Hamaker constant, $\Delta\rho$ is the mass-density difference of the two phases, g is the acceleration of gravity, L is the height of the lower phase [see Fig. 2(b)], and q is given as above. Along the same lines, Dzyaloshinskii *et al.*[3(h)] calculated the long-range interaction of a layered system based on quantum fluctuations. According to their theory, the long-range force can be deduced from the electromagnetic absorption spectra of the components of the wetting system.

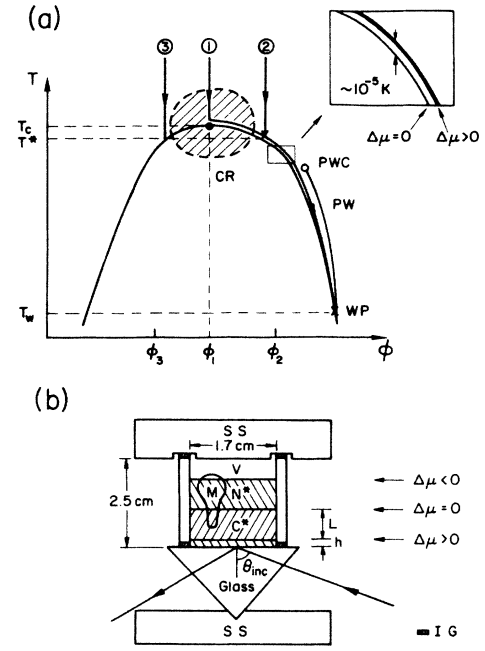

FIG. 2. (a) Phase diagram of the system. φ denotes the volume fraction of carbon disulfide, T the temperature, T_c the bulk critical temperature, T^* the first-order transition temperature, T_w the temperature of the hypothetical wetting transition on coexistence (WP), and CR (shaded region) the bulk critical region. The three thermodynamic trajectories used are labeled by numbers. Placement of hypothetical prewetting (PW) line with prewetting critical point (PWC) on the right-hand side of the phase diagram indicates that the system is wetted by the nitromethane-rich phase. The inset shows how far the system is pushed away form bulk coexistence due to gravity at the surface of the glass substrate along critical trajectory 1, assuming that the system is in thermal equilibrium. The actual distance is probably less due to stirring. (b) Side view of sample cell schematic. V denotes the vapor phase, N^* the nitromethane-rich phase, C^* the carbon-disulfide-rich phase, SS the stainless-steel plates, IG the indium gaskets, h the wetting-layer thickness, and L the height spanned by carbon-disulfide-rich phase (equal to 0.82 cm on trajectory 1). The side wall is a Pyrex glass cylinder. The substrate is a borosilicate glass prism. The cell is held under compression by screws (not shown) connecting the stainless-steel plates. The sample cell seal (not shown) is in the upper stainless-steel plate [see Ref. 2(c)]. M denotes a floating glass-encapsulated magnetic sample mixer. A stainless-steel-enclosed thermostor thermometer (not shown) extended from the top plate into the liquid. $\Delta\mu$ denotes the chemical-potential difference for different levels in the two-phase region. $\Delta\mu$ is taken to be zero at the bulk meniscus and $\Delta\mu > 0$ indicates the right-hand branch of coexistence curve. The line indicates incident light and reflected light. Θ_{inc} denotes the angle of incidence.

On the experimental side, many interesting properties of wetting systems have been revealed. In the paper by Kwon *et al.*[4(a)] the wetting of a vapor "substrate" by binary liquid mixtures was examined. Here, the wetting-layer thickness was measured by ellipsometry. Using a slab model they found that the wetting-layer thickness varied from 7 to 40 nm. Their experiment was consistent with the power-law behavior $h \propto L^{-1/3}$. In the ellipsometric observations of Schmidt and Moldover,[4(b)] a wetting transition was discovered at the liquid-vapor interface of a mixture of C_7F_{14} and C_3H_7OH. Wetting layers between 35 and 50 nm thick were observed. In an independent paper Beaglehole[4(c)] reported a "dewetting" transition at the liquid-vapor interface of cyclohexane and methanol. Complete wetting on the liquid-vapor interface occurred only when a small amount of water was added to the system. By increasing the water concentration, the dewetting temperature T_{on} was shifted to as far as 1 K below the bulk transition temperature T_c. Ross and Kornbrekke[4(d)] also observed dewetting in contact-angle measurements of three different binary liquid systems. Dewetting was found for all the systems when the temperatures were close to T_c. In Ref. 4(d) contact angles between the bulk liquid meniscus and the solid boundaries became 90° upon approaching the critical point, instead of 0° or 180°, as predicted by Cahn's theory.[3(a)] In these studies the dewetting temperatures T_{on} (defined as the temperature at which the contact angle extrapolates to 90°) varied from 30 to 90 mK below T_c. Wetting on a solid boundary was also studied by Moldover and Gammon.[4(e)]. They employed an interferometric tech-

nique to measure the wetting-layer thickness of a one-component fluid, SF_6, as a function of both the temperature and the spatial separation of two optically flat boundaries. Their results can be roughly expressed by saying that close to the bulk critical point the wetting-layer thickness varied as $h \propto (T_c - T)^{-0.3}$. The wetting layer became as thick as 700 nm when the temperature was 2 mK below T_c. No dewetting was found for this liquid-solid system. In a careful experiment performed by Kayser, Schmidt, and Moldover[4(f)] the same liquid system was studied with a simpler geometry, i.e., a single vertical substrate. From ellipsometry measurements they found that the wetting-layer thickness was considerably smaller than in the experiment of Moldover and Gammon. The new results were in quantitative agreement with the theory of Dzyaloshinskii *et al.*[3(h)] At the same time, they reported the discovery of dramatic temperature-gradient effects and local laser-heating effects for this one-component system. Wetting on a single vertical glass plate in binary liquid mixtures was also reported by Law.[4(g)] A thick wetting layer of about 200 nm was found for a cyclohexane-aniline system. For his cyclohexane-methanol system it was even thicker. Recently, Beysens and Estéve have observed aggregation phenomena of silica spheres in the water + 2,6-lutidine system which may suggest a prewetting transition.[4(h)]

In our experiment we combined an acid treatment and vacuum baking to produce glass substrates with hydroxylated surfaces which were attractive to the nitromethane-rich phase (as seen in our earlier critical adsorption measurements,[2] $H_1 < 0$ in this case). As is schematically shown in Fig. 2(b), in the present work we studied the horizontal wetting layer at the bottom of the sample cell. Three thermodynamic trajectories were chosen for this experiment, as shown in Fig. 2(a) and detailed in Table I. Along trajectory 1 the system approached bulk coexistence with the bulk field $H\,(=\Delta\mu - \Delta\mu_c) = 0$ (where $\Delta\mu$ is the difference in the chemical potential per molecule of the two components and c denotes the critical point. We take $\Delta\mu_c = 0$ to simplify notation) at the bulk meniscus, but $H = \Delta\mu \propto \Delta\rho g L > 0$ at the bottom of the cell. Because of this gravity field the thermodynamic trajectory of the bottom of the cell was pushed away from bulk coexistence, as shown in the inset of Fig. 2(a). Using a classical Landau-Ginzburg free energy for the bulk system, we calculated the deviation to be $< 10^{-5}$ K in temperature. It is shown by Kayser, Moldover, and Schmidt[1] that if we take the stirring into account the deviation is another factor of 10^{-2} smaller. Along trajectory 2 the system approached coexistence with $H = \Delta\mu > 0$ (in the single-phase region the system was now richer in carbon disulfide than it was on trajectory 1). For trajectory 2 the bulk field H went to zero linearly with temperature as the coexistence curve was approached (see Appendix A). Along trajectory 3 the system was richer in nitromethane, corresponding to $H = \Delta\mu < 0$ in the single-phase region.

TABLE I. Sample parameters. See text for uncertainties. Trajectory 1 is for cell no. 2.

Trajectory	Carbon disulfide volume fraction	Total volume (ml)	Bulk transition temperature (°C)
1	0.6014	3.326	63.264
2	0.7333	3.409	62.089
3	0.3986	4.254	62.383

Very different wetting behavior was discovered along these three trajectories. By measuring the reflectivity of the liquid-solid interface at the bottom of the cell we find the following: (1) Complete wetting is not a simple continuation of adsorption near the bulk critical point. While a short-range substrate-liquid interaction is sufficient to explain critical adsorption, a long-range substrate-liquid interaction plays an essential role for complete wetting. A dewetting transition is found between 60 and 150 mK below T_c. (2) The thickness of a wetting layer in the single-phase region off the critical concentration is governed by a van der Waals force. (3) We show that gradual temperature gradients and local laser-heating effects are not as severe as in the one-component system of Ref. 4(f).

Our observations are consistent in several qualitative respects with the earlier work discussed above.[4(a)–4(h)] However, the absolute thickness of the wetting layer produced at coexistence is considerably greater than that seen in certain other gravity-thinned experiments.[4(a)–4(c),4(f)] It is also thicker, as is discussed below, than the theoretical value expected for a nonretarded van der Waals force. Kayser *et al.*[1] give an explanation of how this can arise via the effect of sample stirring, which effectively lowers the position of the bulk-liquid–liquid meniscus for trajectory 1, therefore decreasing L in Eq. (1). Along coexistence (trajectory 1), mixing attenuates the effect of gravity by transporting nitromethane-rich material from the upper liquid phase to the bottom of the cell. Off coexistence, in the bulk one-phase region (trajectories 2 and 3), there is no high-density reservoir of nitromethane, since the bulk sample is homogeneous. Therefore, we assert that the wetting behavior observed off coexistence (trajectories 2 and 3) corresponds to that which would be encountered in a gravity-free environment.

This paper is organized in the following way. In Sec. II experimental techniques are discussed, including descriptions of sample preparation, experimental setup, and methods, and in Sec. III data analysis and interpretations are given. The final section contains our conclusions.

II. EXPERIMENTAL TECHNIQUE

A. Sample preparation

As shown in Fig. 2(b), the sample cell consisted of an optical-quality borosilicate glass prism, a Pyrex glass cylinder, and a stainless-steel top plate. Indium gaskets were used as seals. All stainless-steel joints were welded. The sample was sealed, as in Fig. 2 of Ref. 2(b), with a stainless-steel fitting and an aluminum gasket. We followed standard cleaning procedures for glass parts and stainless-steel parts.[5(a)] For glass parts we used chromic acid first and then proceeded with boiling and rinsing with distilled water followed by acetone and methanol.

For stainless-steel parts we used 35 vol % nitric acid, then rinsed them with distilled water thoroughly. All parts were dried by vacuum baking at 170 °C for 12 h, in order to remove physisorbed water. The sample cells were assembled and filled with liquids in an argon dry box. 99 + %-pure nitromethane and carbon disulfide[5(b)] were used without further purification. The critical samples (trajectory 1) typically had a bulk transition temperature of $T_c = 63.2 \pm 0.2$ °C (uncertainty due to variation between samples), consistent with our other experiments[2] (the same visual technique was used), but about 1.2 K higher than the measurements of Gopal, *et al.*[5(c)] This discrepancy is possibly due to small amounts of impurities present in our samples. An overall T_c drift of about + 2 mK/d was observed in the samples with the critical concentration. In order to understand this drift, we measured T_c as a function of time in critical liquid samples sealed in glass ampules along with pieces of stainless steel. T_c drifts comparable to that seen in our wetting cells were observed, while no significant drifts were seen for pure liquid mixtures. We therefore suggest that the T_c drifts seen in our wetting cell were due to slow chemical reactions of liquid mixtures with the stainless-steel components. Near the critical point, these trajectory-1 samples showed a bulk meniscus which remained at the center of the cell (< 0.1 mm change) as the samples were lowered in temperature below the transition temperature, indicating that the concentrations were close to critical. As seen in Table I, the off-critical samples were prepared with the bulk transition temperature T^* being about 1 °C below T_c.

B. Apparatus

The basic experimental setup is similar to our earlier experiments,[2] with the temperature regulated by an improved water bath. Temperature stability was better than 0.2 mK/week. Our thermistor thermometry was automated by a computer-balanced ratio transformer bridge and had a temperature resolution of 0.1 mK. The reflectance was monitored automatically by the same computer. Our reflectance stability at the maximum reflectance was 0.3%/d. The light source was a 1.8-mW He-Ne laser which projected a 1-mm-diam beam on the sample cell.

C. Experimental methods

The reflectivity measurement was performed using frustrated total internal reflection, i.e., the electromagnetic wave inside the wetting layer is an inhomogeneous wave (the E field decays exponentially normal to the surface), while in the rest of space it is a traveling wave. This required an angle of incidence in the neighborhood of the critical angle (78° for our glass substrate with index of refraction $n_{\text{glass}} = 1.515\,09$, as quoted by the manufacturer). For calibration purposes, we measured the maximum reflectance by quenching the system deeply into the two-phase region. The quench-formed wetting layer then gave a saturation of the reflectance, which we took to correspond to 100% reflectivity. The experimental data were taken by monitoring the reflected light constantly until it stabilized as in Fig. 1. A floating glass magnetic mixer, which had a spacing of 1 to 3 mm between its tip and the substrate, continuously stirred the liquid at a rate between 1 and 5 Hz during the observations.

The index of refraction of the carbon-disulfide–rich (C^*) phase at $T < T_c$ was determined by heating the system rapidly (about 70 mK/min for temperatures a few degrees below T_c), so that the wetting layer was burnt off and the glass substrate was in direct contact with the C^* phase. The index of refraction for $T > T_c$ was found at fixed temperature for high temperatures, where no significant critical adsorption occurs[2(a),2(b)] [see Fig. 3(a)]. These two measurements of the bulk background reflectivity gave consistent values for the bulk index of refraction at the critical point.

As stated above, we performed our experiments with three different overall chemical concentrations, which correspond to the three trajectories shown in Fig. 2(a).

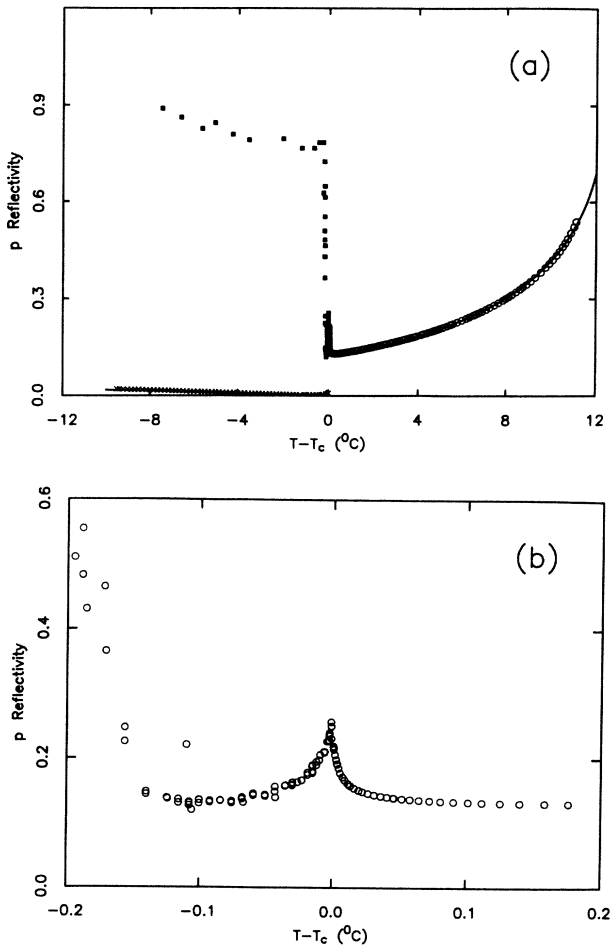

FIG. 3. (a) Reflectivity along trajectory 1 (critical concentration). Incident angle is 1.347 rad. Open circles are the bulk background measurements for $T > T_c$ and crosses are the bulk background measurements for $T < T_c$. Solid squares are the wetting observations. See text for details on how background measurements were obtained. Fitting lines are also discussed in the text. (b) Reflectivity along trajectory 1 near bulk criticality. Incident angle is 1.347 rad. The cusp is due to critical adsorption. The increase in reflectivity near $T - T_c = -0.15$ K indicates the growth of the wetting layer on the glass substrate with decreasing temperature.

Trajectory 1 was for the system at a critical concentration $\varphi_1=\varphi_c=0.601\pm0.002$ (defined by volume fraction of carbon disulfide) given by Ref. 5(c). Strong critical opalescence was seen as the system approached the bulk critical point T_c. Trajectories 2 and 3 were far from bulk criticality, see Table I, in order to simplify the development of the wetting layer as the system approached the coexistence curve. These samples were prepared with an uncertainty of less than 1% in φ. We observed a strong indication (precursor) of wetting with trajectory 2, but there was no such precursor as the system approached the coexistence curve along trajectory 3.

The wetting layer along trajectories 1 and 2 appeared to be smooth at the center of the sample cell. Unlike wetting at the liquid-vapor interface [see Ref. 4(a)], we did not observe pendant drops at our liquid-solid interface. We also checked for wetting-layer irregularities for trajectory 1 at 70 mK below T_c by repeating the reflectivity observations with a range of detector angular acceptances ranging from 2.8 to 10.0 mrad. Significant wetting-layer irregularities would change the "reflectance" for these different samplings of small-angle scattering. The laser collimation was 1.3 mrad. Since no change in the reflectance was observed with the various apertures, we conclude that no significant small-angle scattering was observable, i.e., no significant departures from a flat interface were noticed over the spatial wavelength range 0.13 to 0.45 mm.

The bulk critical temperature was determined by visual observation[2] to better than 1 mK. The first-order bulk transition temperature T^* for trajectories 2 and 3 could be determined to ±10 mK by observing the bulk cloud point. In analyzing our data, we used the maximum slope in the reflectivity as an indication of the bulk transition for trajectories 2 and 3. Within the experimental uncertainties, this was in agreement with the cloud-point measurements.

III. DATA ANALYSIS AND INTERPRETATION

To calculate the wetting-layer thickness along the three trajectories, we used a two-parameter fit to the background reflectivity. For $T<T_c$ the indices of refraction for the C^* and N^* phases were modeled as

$$n^2_{C^*,N^*}=n_0^2\pm AB\,|\,t\,|^{\beta}/2\ , \tag{2}$$

where the $+$ sign is for the C^* phase, the $-$ sign is for the N^* phase, $B=1.64$ is the order-parameter amplitude, and $\beta=0.32$ is the order-parameter exponent.[5(c)] n_0 and A are fitting parameters, and $t=(T-T_c)/T_c$ (T and T_c in K) is the reduced temperature. As a check on the constant term n_0, we modeled the index of refraction n_{bg} for $T>T_c$ by

$$n_{bg}=n_0-at\ , \tag{3}$$

where a is the bulk thermal-expansion coefficient. The fits are shown in Fig. 3(a). These fits gave $n_0=1.4854\pm0.0001$ for $T-T_c<-0.15$ K and $n_0=1.485\,39\pm0.000\,05$ for $T-T_c>0.2$ K. We extrapolate these fits to the critical region to cover the entire temperature range of the experiment. A similar fit was applied to trajectory 2, Fig. 5(a). All the results are listed in Table II. The parameters can be compared with Lorenz-Lorentz calculations, see Appendix B and Ref. 2(c), which are listed in Table III. The calculation is based on knowledge of the thermal-expansion coefficients[6] of each individual liquid. The agreement is excellent for a and A along trajectory 1 and fair for a along trajectory 2. In what follows, we discuss our results for these three trajectories.

A. Trajectory 1: Wetting near coexistence (critical concentration)

In this case, the system approached and followed bulk coexistence with the critical concentration. Reflectivity data are shown in Figs. 3(a) and 3(b). By assuming a symmetrical coexistence curve and using the above fitting parameters (Table II) in Eq. (2), we reduced our reflectivity data to layer thickness with a dielectric slab model. It should be emphasized that our measurement of the wetting layer thickness for $T-T_c>-0.15$ K relies on an extrapolation of the fit to Eq. (2). Four distinct regions can be identified easily from Figs. 4(a)—4(c).

1. Region (i): $T-T_c<-3$ K

The wetting-layer thickness is almost independent of temperature. This is characteristic of the gravity-thinned wetting predicted by de Gennes[3(f)] and Lipowsky.[3(g)] In this temperature range, sample stirring caused the bulk-liquid—liquid interface to wave, but did not break it up. As suggested by Lipowsky,[3(g)] we calculated the sign of the Hamaker constant for our system using the long-range part ($1/r^6$) of a Lennard-Jones potential. Assuming that the long-range interaction between any pair of liquid molecules is equal and that the long-range interaction between either liquid molecule and a substrate molecule unit is equal, then the Hamaker constant can be written as

$$W=\pi(e_{ll}n_{N^*}-e_{ls}n_S)(n_{C^*}-n_{N^*})/12\ , \tag{4}$$

where the n's are the number densities of each species (S denotes substrate), e_{ll} is the liquid-liquid molecular interaction parameter and e_{ls} is the liquid-substrate molecular interaction parameter. For our system, assuming that e_{ls} is the same as e_{ll} and since $n_S>n_{N^*}$ and $n_{N^*}>n_{C^*}$

TABLE II. Experimental parameters for bulk dielectric constants. See text for definitions.

Trajectory	φ	n_0	a	A
1	0.6014	1.485 39±0.000 05	0.221±0.030	0.75±0.05
2	0.7333	1.517 26±0.000 05	0.307±0.030	

TABLE III. Lorentz-Lorenz calculation of bulk dielectric parameters. See text for definitions.

Trajectory	φ	a	A
1	0.6014	0.220	0.77
2	0.7333	0.238	0.77

[see Ref. 7(a)], we have $W>0$. This implies that the interaction between the liquid-liquid interface and the liquid-substrate interface is repulsive, thereby favoring a thick wetting layer. Also, because the mass-density and number-density differences have the same temperature dependence, Eq. (1) predicts constant layer thickness h, independent of temperature. Qualitatively, our results agree with this prediction of the long-range force theory of de Gennes[3(f)] and Lipowsky.[3(g)]

In order to estimate the wetting-layer thickness, we evaluate the Hamaker constant according to a nonretarded van der Waals interaction[3(h)]: $W=\hbar\bar{\omega}/16\pi^2$, where $\hbar\bar{\omega}$ is a characteristic energy for the electromagnetic absorption spectra of the three materials (nitromethane, carbon disulfide, and borosilicate glass) involved. Since the ionization energies of the component elements are all less than 14 eV,[6] we assert that $\hbar\bar{\omega}<14$ eV. This, in turn, gives $W<1.5\times10^{-13}$ erg. We can apply Eq. (1) with a $\Delta\rho$, the density difference of the pure fluids, of 0.14 gm/cm^3,[6] $g=980$ cm/sec^2, and L, the "physical" height of the C^*

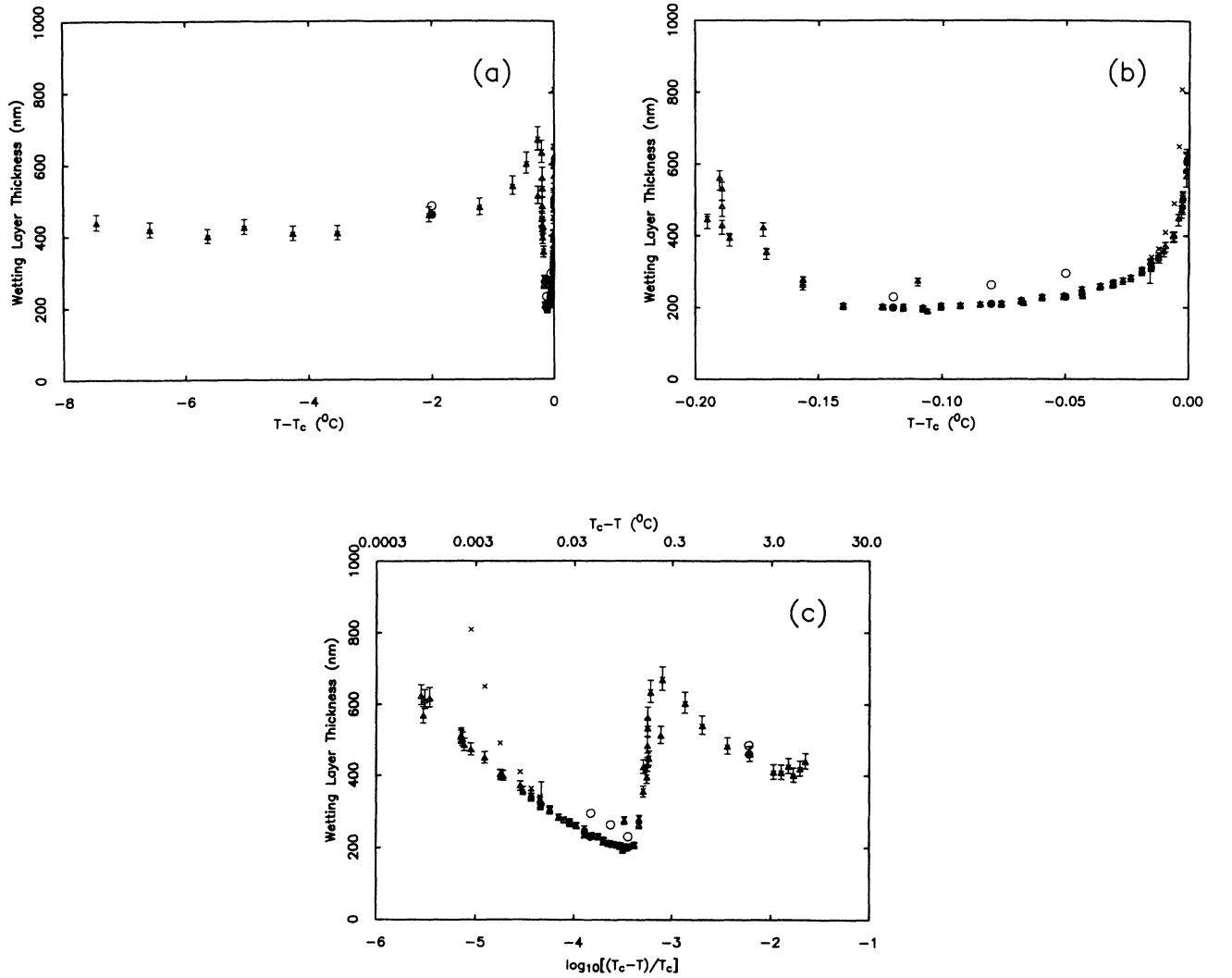

FIG. 4. (a) Wetting-layer thickness calculated by the slab model for trajectory 1 (cell no. 2 at critical concentration). Triangles indicate thickness according to the slab-model calculation. Uncertainties in thickness are derived from uncertainties in the reflectivity. Crosses are discussed in (b). Circles indicate laser-heating tests with cell no. 3. Open circles indicate the measured thickness when the laser power is reduced by a factor of 4. Solid circles are measurements with full laser power. The laser-heating data (solid circles) are normalized to agree with the measurements for cell no. 2. (b) Wetting-layer thickness near bulk criticality for trajectory 1 (cell no. 2). Triangles indicate thicknesses according to the slab model. Crosses are calculated by a hyperbolic-tangent dielectric profile with effective diffuseness equal to 4 times the bulk correlation length. Circles indicate laser-heating effects as in (a). (c) Semilogarithmic plot of wetting-layer thickness versus the reduced temperature (cell no. 2). All the symbols are identical to those in (a). The dewetting transition is clearly seen for $T_c-T=0.15$ K.

phase, equal to 0.82 cm. The resultant upper limit on h, 140 nm, is considerably thinner than we have observed in region (i). Therefore, we take the suggestion made by Kayser *et al.*[1] that stirring reduces the effective L in Eq. (1).

For trajectory 1 we tried three different cells, presumably prepared under identical conditions, but we found that in region (i) the layer thickness varied from 400 to 600 nm for the different cells. Each individual cell gave reproducible results. We suspect that the discrepancy could be a result of different stirring conditions between different cells. The results displayed in the figures of this paper are for our cell no. 2. Cell no. 1 showed a slight discoloration after three months of observation and fits to the bulk background reflectivity were not satisfactory. We suspect that it had a leak. Cell no. 2 showed no discoloration over the course of the experiment (more than three weeks) and give excellent fits to the bulk background reflectivity as discussed above. Cell no. 3 was used for about two weeks for experiments on gradual temperature gradients and local laser heating effects, which will be discussed next.

As reported recently by Kayser, Schmidt, and Moldover,[4(f)] sample temperature gradients arising from gradual thermal inhomogeneities in the cell and local laser heating can significantly change the wetting behavior of a one-component liquid-vapor system. As these authors explain, when a temperature gradient perpendicular to the substrate is applied, the wetting-layer thickness is determined by the balance between condensation and draining effects. We checked for gradual temperature-gradient effects in region (i) by installing a pair of heating coils on the top and bottom of the stainless-steel plates of the sample cell. These heaters allowed us to introduce a temperature gradient of about 1.0 mK/cm in either direction. A differential copper-Constantan thermocouple pair was attached to the outside wall of the sample cell. Without applied heat, the temperature gradient was <0.5 mK/cm (measurement limited by the sensitivity of the thermocouple) on the side wall of the cylinder. Removing the sample cell from the water bath, we were able to measure gradients in the water bath with high sensitivity by using a movable thermistor probe and a fixed quartz-thermometer reference. This gave a gradient value <0.1 mK/cm. Only a very small change, $+$ $(-)3\%$, in layer thickness was observed as we applied a temperature gradient of $-$ $(+)$ 1 mk/cm in region (i) (where $-$ represents a temperature increase from the bottom of the cell to the top of the cell and vice versa). Since the gradient we applied was much larger than that normally present in the system, we conclude that gradual temperature gradients were not important in region-(i) measurements.

We did, however, find that laser heating had a noticeable effect in our system. By using a pair of crossed polarizers to vary the incident laser power, we measured the wetting-layer thickness in region (i) for different incident light intensities. With a laser operated at full power (rated at 1.8 mW), the wetting-layer thickness was about 10% thinner than when the laser operated at $\frac{1}{4}$ of its full power, as shown by the circles in Fig. 4(a). Upon further decrease in light intensity, the wetting-layer thickness was not affected. We checked for this by blocking the incident laser beam for many hours, thereby allowing the wetting layer to recover its steady-state thickness. Running the beam at $\frac{1}{4}$ power, the initial reflectance upon exposing the sample to light was compared with the measurement after a period of 4 h. For the different temperature regions, no significant difference could be found between these two measurements, unlike the situation with full laser power.

In exploring the lowest temperatures available in our thermostat, we did not observe a transition from complete to partial wetting in the system, even though the temperature was extended to 20 K below T_c. Our equilibrium capillary-rise measurements[7(a)] with a hydroxylated substrate show that the transition temperature is at least 14 K below T_c. Our nonequilibrium capillary-rise experiments suggest that it is at least 73 K below T_c if the transition exists. This is to be compared with the discoveries of partial to complete wetting transitions in binary liquid mixtures by Pohl and Goldburg,[7(b)] Schmidt and Moldover,[4(b)] and Beaglehole,[4(c)] at approximately 15, 52, and 34 K below T_c, respectively.

2. *Region (ii): $-200\ mK > T-T_c > -3\ K$*

As shown in Figs. 4(a) and 4(c), the layer thickness increased as the system approached the bulk critical temperature. The total increase of the layer thickness was about 40%. A power-law fit in this region yields an exponent 0.55 ± 0.20. Such an increase in layer thickness is not uncommon. For example, Kwon *et al.*[4(a)] and Beaglehole[4(c)] found the same behavior for wetting on a liquid-vapor interface, and Moldover and Gammon[4(e)] observed such thickening for wetting on a liquid-solid interface.

3. *Region (iii). $-150\ mK > T-T_c > -200\ mK$*

As shown in Figs. 4(a)—(4c), the layer thickness dropped rapidly in this temperature range to about half of its low-temperature value [region (i)]. Since we were close to bulk criticality, the slab model may no longer be a good approximation. Following the suggestion of Widom, we considered the importance of the enhanced thickness (diffuseness) of the liquid-liquid interface near the critical point. We employed a model for the wetting layer with a classical hyperbolic-tangent profile for the dielectric constant,

$$n^2(z)=\{(n_{C^*}^2+n_{N^*}^2)+(n_{C^*}^2-n_{N^*}^2)\times\tanh[2(z-h)/n\xi]\}/2\ , \tag{5}$$

where $n\xi$ is the width of the liquid-liquid interface. For this particular profile, Huang and Webb[8] showed that if one requires the perturbation far from the liquid-liquid interface to fall off in an exponential manner with the decay length proportional to the bulk correlation length ξ, then $n=4$, i.e., the effective diffusive width of the liquid-liquid interface should be 4 times the bulk correlation length. A numerical solution to Maxwell's equations was used to find the reflectivity exactly.[9] The results are shown in

Figs. 4(b) and 4(c). Since the deviations from the slab-model calculation only appear significant as close as 20 mK below T_c, we conclude that the sudden drop in layer thickness near $T_c - T = 150$ mK is not due to critical interface diffuseness. This result is reminiscent of Beaglehole's ellipsometric reflected-light observations[4(c)] and the contact-angle work of Ross and Kornbrekke.[4(d)] Beaglehole called this liquid-mixture phenomenon "dewetting." It is characterized by the onset temperature T_{on} ($T_w < T_{on} < T_c$),where complete wetting was suddenly suppressed. In our experiment, we found that dewetting occurred at different temperatures, ranging from 60 to 150 mK below T_c for different sample cells. We suspect that the discrepancy is due to different stirring conditions or differing small amounts of impurities in the system.

Dewetting was interpreted by Beaglehole as arising from capillary-wave fluctuations on the wetting interface. This argument could be true for a thin wetting layer, such as in Beaglehole's liquid-vapor interfaces, but for our thick wetting layer is is not adequate. The nature of the dewetting transition in our system is still unknown; it might be due to the crossing of the prewetting line, which results in a thin- to thick-layer transition [as pointed out by Lipowsky, this is the reverse of the behavior, a thick-to-thin-layer transition, expected from Ref. 3(b)] or a hydrodynamic instability near the bulk critical point. A third possibility is given by Lipowsky.[10] The long-range part of the free energy, $U(h)$, can be expanded in inverse powers of the layer thickness h beyond that given in Eq. (A1), Appendix A:

$$U(h) = W_3/h^3 + W_4/h^4 + \cdots . \tag{6}$$

Since $W_3 \to 0$ as $T \to T_c$, the higher-order terms may start to dominate in the critical region. These higher-order terms may cause the thinning of the wetting layer. At present, there is no microscopic calculation for the expansion coefficients, W_n. More theory and experiment are needed to test these possibilities.

4. *Region (iv): $150 > T - T_c > -150$ mK*

This was a region of critical adsorption, Fig. 3(b). In this experiment, in addition to the anomalous adsorption of nitromethane molecules to the glass substrate for $T > T_c$, as in Refs. 2(a) and 2(b), we have also observed the anomalous adsorption for $T < T_c$. A clear cusp near the bulk critical point indicated that the order-parameter profile $m(z)$ [$=\varphi(z) - \langle\varphi\rangle$, where $\langle\ \rangle$ indicates averaging over the entire sample] near the wall decays rapidly, as would be qualitatively expected from an exponential profile with a decay length approximately equal to the bulk correlation length.

In this region, for $T < T_c$, the effects of local laser heating are significant. Translating the reflectivity data to layer thickness as shown in Figs. 4(b) and 4(c), the change in the layer thickness is about 25% for the laser operated at full power compared to $\frac{1}{4}$ power. Since the layer thickness is nevertheless small in region (iv) as compared with regions (i) and (ii), we conclude that the dewetting is a real effect.

In summary, for wetting near coexistence, as a function of increasing temperature, we find regions in which the wetting-layer thickness for the stirred system is independent of temperature, then grows with temperature and then abruptly decreases with temperature. Closer to the critical point, the divergent correlation length produces critical adsorption. We investigated nonequilibrium thermal effects due to gradual temperature gradients and local laser heating, but unlike the situation in a one-component fluid,[4(f)] these effects are not dramatic in our system.

B. Trajectory 2: Wetting off coexistence

First of all, we did not see a prewetting transition at this particular concentration,[3(a)] although the temperature resolution was < 1 mK. It was noticed that in the bulk one-phase region, the cooling data and heating data were very consistent [see Figs. 5(a) and 5(b)]. Long relaxation times, presumably due to hydrodynamic effects, seen in

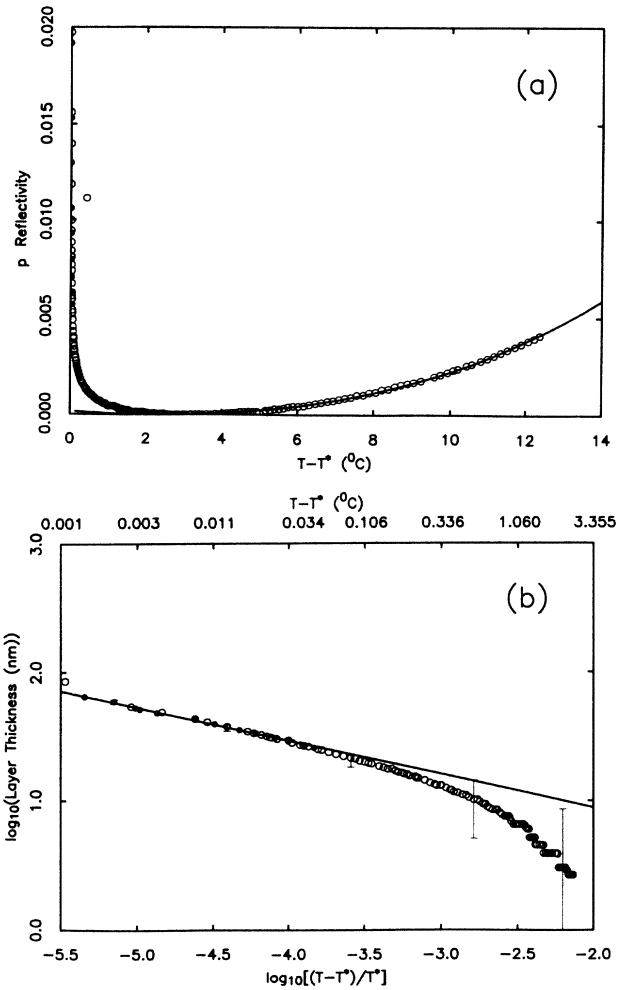

FIG. 5. (a) Reflectivity along trajectory 2, wetting off coexistence. Incident angle is 1.347 rad. Open circles are reflectivity data upon cooling and solid circles are reflectivity data upon heating. The line is the fit to the bulk background reflectivity. T^* is the bulk transition temperature. (b) Wetting-layer thickness calculated by the slab model for trajectory 2. Open circles are cooling data and solid circles are heating data. The line is the fit to the power law described in the text.

trajectory 1 along coexistence, were not noticed for trajectory 2 (single-phase region).

Since the transition temperature T^* was far about (1.2 K) below T_c, we again used the slab model to calculate wetting-layer thickness from reflectivity. A noticeable layer started to build up at $T-T^*=2$ K. A log-log plot of layer thickness as a function of reduced temperature is shown in Fig. 5(b). Asymptotically, the layer thickness as a function of reduced temperature obeys the plotted power law,

$$h=(2.7\pm0.3)[(T-T^*)/T^*]^{-(0.258\pm0.020)}\ \text{nm}\ ,$$

with a rms deviation of 0.006 in the temperature range $T-T^*<0.035$ K. As discussed below, the exponent $-\frac{1}{4}$ is expected for a retarded van der Waals interaction between the liquid and substrate. Our data did not fit well to this exponent for $T-T^*>0.3$ K (which corresponds to $h<20$ nm). We expect that for wetting-layer thicknesses which are much thinner than the wavelength corresponding to significant electromagnetic absorption, the force law should become nonretarded,[3(h)] i.e., exponent equal to $-\frac{1}{3}$. However, in the range $T-T^*>0.3$ K, because of our inadequate knowledge of the index of refraction of a thin wetting film and the fact that the surface signal became exceedingly small compared with the background uncertainties, only in a very small temperature region could the data be reliably fit to the power $q=\frac{1}{3}$. The error bars in Fig. 5(b) were calculated based on the uncertainty in the reflectivity measurements. It should be noted that the exponent found above, for $T-T^*<0.035$ K, is not sensitive to the way we modeled our dielectric constant for the N^* phase, which we assumed to have the same thermal-expansion coefficient as the C^* phase [see Eq. (3) and Table II]. For the data shown in Fig. 5(b), we assumed that the constant part of the wetting layer's index of refraction is chosen to agree with Eq. (2) on coexistence. If we take the index of refraction as a constant for the N^* phase, q only changes by about 3%.

Our approach to bulk coexistence experiment is analogous to multilayer gas-adsorption-on-solid experiments.[11(a),11(b)] In gas-on-solid experiments, if one phenomenologically assumes[3(d)] a strong substrate (i.e., the long-range atom-substrate interactions are stronger than atom-atom interactions) and $\mu-\mu^*\propto T-T^*$,[3(g)] where μ denotes chemical potential per molecule and $*$ denotes coexistence, then the thickness of the adsorbed layer, h, behaves near bulk coexistence as

$$h=[B(T)/(T-T^*)]^{-q}\ , \tag{7}$$

where, in general, $B(T)$ is a nonsingular, temperature-dependent quantity, $q=\frac{1}{3}$ for a nonretarded force, and $q=\frac{1}{4}$ for a retarded force. For a binary liquid mixture off the critical concentration, a similar dependence of wetting-layer thickness on temperature is expected, as shown in Appendix A. We conclude that our thick wetting-layer observations of the approach to coexistence for $T-T^*<0.035$ K are in good agreement with a retarded van der Waals force model for the substrate-liquid interaction.

C. Trajectory 3: Nonwetting off coexistence

As shown in Fig. 6, we do not see a precursor of wetting as for trajectory 2 in Fig. 5(a). This can be understood by the fact that both $H_1<0$ and $H<0$.[3(b)] No sign of increase in reflectivity means no surface enhancement of N^* adsorption or evidence for a "drying" transition (wetting by the C^* phase). The sudden dip in reflectivity with decreasing temperature indicated bulk phase separation. At this point, the heavier C^* phase was separating from the background N^* phase. At first, this new phase formed many tiny droplets on the glass substrate, giving rise to intense scattering of light from the surface. Unlike trajectory 2, these droplets never spread out to form a film; instead, they aggregated to form large droplets, which eventually rolled to the corner of the cell. The reflectivity then recovered its initial high value.

IV. CONCLUSIONS

We have observed gravity-thinned wetting by the nitromethane-rich phase onto a borosilicate glass substrate from a stirred binary liquid mixture of carbon disulfide and nitromethane. From a theoretical point of view, such a liquid state is energetically favorable for our system along trajectories 1 (critical concentration) and 2 (carbon disulfide surplus), because we have a contact surface field with $H_1<0$ [which attracts the nitromethane-rich phase, see Refs. 2 and 7(a)] and a bulk field with $H>0$. For trajectory 1 (critical concentration), gravity provided $H>0$ at the point of observation. For trajectory 2 (carbon disulfude surplus) $H>0$ throughout the sample while the system is in the single-phase region ($T>T^*$). This is as required by the Nakanishi-Fisher phase diagram.[3(b)] If the long-range substrate-liquid force, which favors wetting by the nitromethane-rich phase, is also considered, our system should again have a N^*-phase wetting layer. On the other hand, when the system has $H<0$, as in trajectory 3 (nitromethane surplus) for $T>T^*$, no wetting phenomenon is observed as expected from the Nakanishi-Fisher phase diagram.

Sample stirring plays an interesting role in these experiments. At bulk coexistence, stirring allows us to achieve

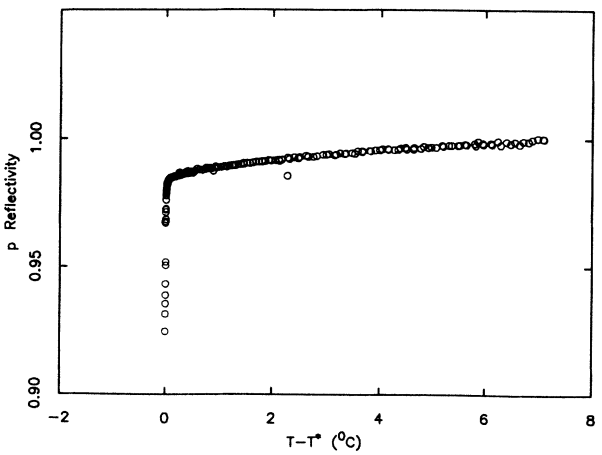

FIG. 6. Reflectivity along trajectory 3, nonwetting off coexistence. Incident angle is 1.301 rad.

wetting layers which assume a steady-state thickness after abrupt changes in the wetting-layer thickness due to heating or cooling. These changes have relaxation times as long as a day. Kayser *et al.*[1] point out that stirring facilitates the formation of this wetting layer by transporting material into gravitationally unfavored regions. For our wetting observations in the bulk single-phase region, the relaxation times are short, so that recovery periods are unnecessary. Since the samples are homogeneous in the bulk, stirring apparently maintains an effectively gravity-free system.

In conclusion, our experiments show the following: (i) At bulk coexistence, complete wetting is not a simple continuation of critical adsorption. For example, dewetting is found near bulk criticality. (ii) Again at bulk coexistence, far away from the bulk critical point, the wetting-layer thickness is 400–600 nm. This remarkably thick wetting layer may be a result of stirring,[1] which greatly reduces the effective bulk gravity field. (iii) In the single-phase region off the critical concentration, the system obeys a retarded van der Waals force for thicknesses greater than 20 nm with an exponent of temperature dependence $q=0.258\pm0.020$ [see Eq. (7)], in agreement with the theoretical prediction $q=\frac{1}{4}$.

ACKNOWLEGMENTS

We want to thank Dr. R. Lipowsky for his generous help and suggestions. We also appreciate the discussions we have had with Professor B. Widom, Professor M. E. Fisher, Dr. M. R. Moldover, and Dr. R. Kayser. In particular, we thank Dr. Moldover and Dr. Kayser for sharing their new results. We also want to thank Dr. M. Schneider and Dr. M. Telo da Gama for their help. We want to thank Professor N. R. Hill and Professor J. Sethna for their invaluable suggestions on the solution of Maxwell's equations. The experimental assistance provided by Mr. Gregory Kellogg, Ms. Carol Federighi, and Ms. Kumudini Abeyaratne is also gratefully acknowledged. Finally, the financial support of the National Science Foundation through the Materials Science Center at Cornell University is appreciated.

APPENDIX A: EFFECTIVE BULK FIELD FOR A NONCRITICAL TRAJECTORY

Following Lipowsky's suggestion, we calculate the surface free energy F_s with classical Landau-Ginzburg free-energy density in an external field H. A linear expansion with respect to H gives

$$F_s=2\varphi^* Hh+W/h^{\sigma}\ , \tag{A1}$$

where φ^* is the order parameter at the transition temperature T^*, h is the wetting-layer thickness, H is the bulk field, and W is the Hamaker constant. For a binary liquid mixture, H measures the closeness of a system to bulk coexistence.[3(b)] In the case of ideal-gas mixtures, H can be evaluated exactly,[12]

$$H=k_B(T-T^*)\ln[(M_1/M_2)^{3/2}P_2/P_1]\ , \tag{A2}$$

where M_1 and M_2 are the molecular weight of the first and second components, P_1 and P_2 are the partial pressures of the first and second components, respectively, and k_B is Boltzmann's constant. Minimizing the surface free energy of (A1) with respect to h, we have the equilibrium layer thickness as a function of temperature:

$$h\propto(T-T^*)^{-q}\ , \tag{A3}$$

with $q=1/(1+\sigma)$. For a nonretarded van der Waals force, $\sigma=2$, and for a retarded van der Waals force $\sigma=3$.[3(g),3(h)]

APPENDIX B: EVALUATION OF THE THERMAL-EXPANSION COEFFICIENT OF THE OPTICAL DIELECTRIC CONSTANT

In order to relate the thermal-expansion coefficient of the optical dielectric constant for our binary liquid mixture to that of each individual component, we use the Lorentz-Lorenz relation[13]

$$f(\epsilon)=f(\epsilon_N)+\varphi[f(\epsilon_C)-f(\epsilon_N)]\ , \tag{B1}$$

where ϵ_N, ϵ_C, and ϵ are the optical dielectric constants of pure nitromethane, pure carbon disulfide, and the mixture, respectively, and φ is the local volume fraction of carbon disulfide.

The function $f(x)$ is given by

$$f(x)=(x-1)/(x+2)\ . \tag{B2}$$

Dielectric constants are related to refractive indices by $\epsilon=n^2=(n_0-at)^2$ for a mixture, where n_0 is a constant. Similar relations hold for each component. Here t is taken as the reduced temperature for the binary liquid mixture. In our case $t=(T-T_c)/T_c$, with $T_c=336.5$ K. By performing a linear approximation for the small thermal expansion over the range of temperature of our observations, we have

$$ag(n)=a_Ng(n_N)-\varphi[a_Ng(n_N)-a_Cg(n_C)]\ , \tag{B3}$$

where the function $g(x)$ is given by

$$g(x)=x/(x^2+2)^2\ . \tag{B4}$$

Using thermal-expansion coefficients for a_N and a_C from Ref. 6, we find $a=0.22$ for a critical mixture (traectory 1, $\varphi_1=0.601$) and $a=0.24$ for one noncritical mixture (trajectory 2, $\varphi_2=0.733$).

[1]R. F. Kayser, M. R. Moldover, and J. W. Schmidt, in *Proceedings of the Farady Society Symposium on Wetting* (unpublished).

[2](a) C. Franck and S. E. Schnatterly, Phys. Rev. Lett. **48**, 763 (1982); (b) M. Schlossman, Xiao-lun Wu, and C. Franck, Phys. Rev. B **31**, 1478 (1985); (c) J. A. Dixon, M. Schlossman, Xiao-lun Wu, and C. Franck, *ibid.* **31**, 1509 (1985).

[3](a) J. W. Cahn, J. Chem. Phys. **66**, 3667 (1977); (b) H. Nakanishi and M. E. Fisher, Phys. Rev. Lett. **49**, 1565 (1982); (c) V. Privman, J. Chem. Phys. **81**, 2463 (1984); (d) R. Pandit, M. Schick, and M. Wortis, Phys. Rev. B **26**, 5112 (1982); (e) P. G. de Gennes, C. R. Acad. Sci. (Paris) **297**, 9 (1983); (f) P. G. de Gennes, J. Phys. (Paris) Lett. **42**, L377 (1981); (g) R. Lipowsky, Phys. Rev. B **32**, 1731 (1985); (h) I. E. Dzyaloshinskii, E. M. Lifshitz, and L. P. Pitaevskii, Adv. Phys. **10**, 165 (1961).

[4](a) O'D. Kwon, D. Beaglehole, W. W. Webb, B. Widom, J. W. Schmidt, J. W. Cahn, M. R. Moldover, and B. Stephenson, Phys. Rev. Lett. **48**, 185 (1982); (b) J. W. Schmidt and M. R. Moldover, J. Chem. Phys. **79**, 379 (1983); (c) D. Beaglehole, J. Phys. Chem. **87**, 4749 (1983); (d) S. Ross and R. E. Kornbrekke, J. Colloid Interface Sci. **98**, 446 (1984); (e) M. R. Moldover and R. W. Gammon, J. Chem. Phys. **80**, 528 (1984); (f) R. F. Kayser, J. W. Schmidt, and M. R. Moldover, Phys. Rev. Lett. **54**, 707 (1985); (g) B. M. Law, Phys. Rev. B **32**, 5996 (1985); (h) D. Beysens and D. Estéve, Phys. Rev. Lett. **54**, 2123 (1985).

[5](a) F. Rosebury, *Handbook of Electron Tube and Vacuum Techniques* (Addison-Wesley, Reading, 1965), p. 5; (b) Stock Nos. 23071-1 and 15470-9, Aldrich Chemical Company, Milwaukee, WI; (c) E. S. R. Gopal, R. Ramachandra, P. Chandra Sekhar, K. Govindarajan, and S. V. Subramanyam, Phys. Rev. Lett. **32**, 284 (1974).

[6]Thermal-expansion coefficients and densities for pure carbon disulfide and nitromethane can be found in *Handbook of Chemistry and Physics,* 63rd ed. (Chemical Rubber Co., Boca Raton, FL, 1983) and in E. E. Toops, Jr., J. Phys. Chem. **60**, 304 (1956), respectively. Elemental ionization potentials are from the former.

[7](a) K. Abeyaratne, Xiao-lun Wu, and C. Franck (unpublished). In this paper, the approximate molecular number densities for the pure liquids are quoted. At 25 °C, they are, respectively, 1.11×10^{22} and 1.00×10^{22} cm^{-3} for nitromethane and carbon disulfide (see Ref. 6), and 2.2×10^{22} cm^{-3} for borosilicate glass; see G. W. Morey, *Properties of Glass* (Reinhold, New York, 1938), pp. 23 and 85; (b) D. W. Pohl and W. I. Goldburg, Phys. Rev. Lett. **48**, 1111 (1982).

[8]J. S. Huang and W. W. Webb, J. Chem. Phys. **50**, 3677 (1969).

[9]C. Franck (unpublished).

[10]R. Lipowsky (private communication).

[11](a) J. Krim, J. G. Dash, and J. Suzanne, Phys. Rev. Lett. **52**, 640 (1984); (b) C. E. Bartosch and S. Gregory, *ibid.* **54**, 2513 (1985).

[12]E. M. Lifshitz and L. P. Pitaevskii, *Statistical Physics,* 3rd ed. (Pergamon, Elmsford, 1980), Pt. 1, pp. 134 and 282.

[13]S. H. Maron and C. F. Prutton, *Principles of Physical Chemistry,* 4th ed. (Macmillan, New York, 1968), p. 693.